Relationship between Carotid Computed Tomography Dual-Energy and Brain Leukoaraiosis

Luca Saba, MD,* Roberto Sanfilippo, MD,† Antonella Balestrieri, MD,* Fulvio Zaccagna, PhD,‡ Giovanni Maria Argiolas, MD,§ Jasjit S. Suri, PhD, MBA, fellow AIMBE,‖ and Roberto Montisci, MD†

Background: The purpose of this study was to assess if there is a correlation between the carotid computed tomography (CT) Hounsfield unit (HU)-based plaque attenuation values measured using dual-energy CT (DECT) scanner and brain leukoaraiosis (LA). *Methods:* Fifty consecutive patients (34 males, 16 females; mean age, 69 years; age range, 46-84 years) who underwent carotid CT and brain magnetic resonance imaging were included in the study. CT examinations were performed with a DECT scanner, and LA lesion volume quantification was performed using a semiautomated segmentation technique. *Results:* We found an inverse statistically significant correlation between the HU-based carotid artery plaque attenuation and the LA lesion volume. Because of the presence of calcified plaques, a second model was calculated at low kiloelectron volt levels from 66 to 100 and 100 kV by taking into consideration the fatty and mixed plaques, and this further led to the associations between HU-based attenuation and LA volume in brain and vascular territories. *Conclusions:* The results of our study suggest that the associations between HU attenuation of the carotid artery plaques (with the exclusion of calcified plaques) and the volume of LA are emphasized at low keV energy levels.
Key Words: Carotid—CT—dual-energy CT—leukoaraiosis.

Introduction

In recent years, computed tomography (CT) imaging has benefited from the addition of dual-energy CT (DECT) technology, which relies on multilevel kiloelectron volt (keV) dataset acquisition, thereby allowing the study of body tissues in several new ways.[1-4] In particular, in the study of the carotid artery plaque, some preliminary studies have demonstrated that the Hounsfield unit (HU) values of plaque may significantly change according to the selected keV volt; this means that the HU-based plaque type (fatty, mixed, calcified) should be classified according to the energy level applied[5] (Fig. 1).

Leukoaraiosis (LA) is a condition frequently observed in older individuals, and the prevalence of this condition ranges between 8% and 28%, and 90% of subjects aged 80 years and older have some degree of LA.[6-8] This condition is important because it is associated with increased risk of stroke, brain hemorrhage, and depression, and therefore there is a growing interest in the detection and characterization of this condition.[9,10]

The pathogenesis of LA is not completely understood, but most authors hypothesize that this condition is mostly due to cerebral ischemic small-vessel disease.[11]

From the *Department of Radiology, Azienda Ospedaliero Universitaria (A.O.U.), Cagliari 09045, Italy; †Department of Vascular Surgery, Azienda Ospedaliero Universitaria (A.O.U.), Cagliari 09045, Italy; ‡Department of Radiology, University of Cambridge School of Clinical Medicine, Cambridge, CB2 0QQ, UK; §Department of Radiology, AOB, Cagliari, Italy; and ‖Stroke Diagnostic and Monitoring Division, AtheroPoint LLC, Roseville, CA, USA.

Received November 12, 2016; revision received March 27, 2017; accepted April 14, 2017.

Address correspondence to Luca Saba, MD, Department of Radiology, Azienda Ospedaliero Universitaria (A.O.U.), di Cagliari—Polo di Monserrato s.s. 554 Monserrato, Cagliari 09045, Italy. E-mail: lucasaba@tiscali.it.

1052-3057/$ - see front matter

http://dx.doi.org/10.1016/j.jstrokecerebrovasdis.2017.04.016

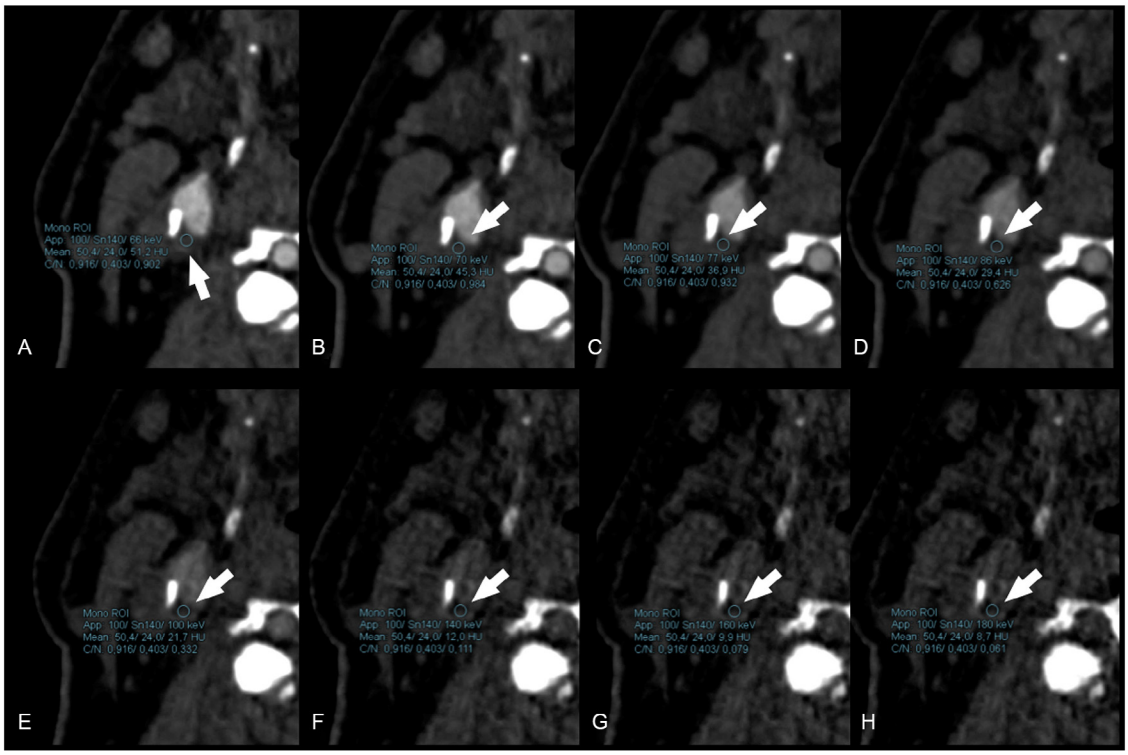

Figure 1. *Screenshots of the carotid artery plaque of a 63-year-old male subject who underwent carotid artery analysis. The HU attenuation values for 66, 70, 77, 86, 100, 140, 160, and 180 keV are given in panels A–H respectively as visible in the ROI* (white arrows)*. The attenuation of 100 and 140 kV are given in each panel. Abbreviations: HU, Hounsfield unit; ROI, region of interest.*

However, recent published papers have linked this condition to large-vessel atherosclerosis.[12-14]

Because of the potential association between carotid artery pathology and LA, we tried to explore the potential correlation between the volume of LA and the carotid artery plaque attenuation by considering the different HU levels owing to the different keV selection obtainable with the dual-energy scanner.

Therefore, the purpose of this study was to assess if there is a correlation between the carotid CT plaque attenuation values measured with DECT scanner and brain LA.

Materials and Methods

Study Design and Patient Population

In accordance with the applicable National Research Ethics Service guidance, ethical approval for the study was not required because the study was performed retrospectively on routinely acquired images, and patients' consent was waived. Fifty (34 males, 16 females; mean age, 69 years; age range, 46-84 years) consecutive patients who underwent DECT of carotid artery vessels and brain magnetic resonance imaging (MRI) were included. Analysis of the database was performed from January 2013 to February 2014.

The inclusion criteria to acquire CT of carotid arteries were (1) ultrasound finding of significant stenosis or a plaque's alteration (irregular surface, intra-plaque hemorrhage, ulceration in the plaque); and (2) when ultrasound could not adequately assess the degree of stenosis and the plaque type. We considered the following exclusion criteria: (1) presence of cerebral strokes (large-vessel infarcts); (2) other pathological conditions that involve the white matter such as demyelinating diseases, connective tissue diseases, and vasculitis; and (3) other pathologies of the brain (neoplasms, abscess, encephalitis). None of the patients included in the study had a medical history of reduced cardiac output or heart failure, as reported in the electronic medical record. A fourth exclusion criterion was the time frame between DECT and MR > 3 months.

CT Technique

All patients were analyzed using a multidetector CT scanner (SOMATOM Definition Flash, Siemens, Berlin, Germany) according to a previously reported technique.[5] In summary, angiographic phase was obtained by injecting 60 mL of contrast medium (Ultravist 370; Bayer Schering Pharma AG, Berlin, Germany) using a power injector at a flow rate of 5 mL/s and an 18-gauge intravenous catheter. To calculate the correct timing of the CT acquisition, a smart prep technique was used by injecting 15-mL bolus of contrast medium to synchronize the data acquisition. Angiographic acquisition was performed in caudocranial direction from the aortic arch to the carotid siphon.

Image Reconstruction and Plaque Analysis

Images were reconstructed on a dedicated workstation with GSI software (Advantage Windows Workstation version 4.4, GE Healthcare, Niskayuna, NY), and from the CT raw data, multiple datasets were generated at the following monochromatic energy levels: 66, 70, 77, 86, 100, 140, 160, and 180 keV, and further with 100 and 140 kV. To quantify the HU attenuation values, 2 radiologists (L.S. and A.B.) performed independently the measurements using a circular or elliptical region of interest (ROI; ≥2 mm^2) in the thickest area of the plaque. To calculate the HU values in the other datasets, the option "propagate" was applied to place the same ROI (morphology and area) in the same topographical position of the plaque.

According to the classification proposed by de Weert et al,[15] it is possible to identify different plaque components based on the attenuation values (fatty plaques are those with an HU value < 60 HU, fibrous plaques are those with an HU value between 60 and 130 HU, and calcified plaques are those with an HU value > 130 HU).

MR Imaging Technique

Brain MR examinations were performed according to an HDxt 1.5T MRI Scanner (GE, Niskayuna, NY) with an 8-channel head coil. As part of the brain protocol, axial and sagittal 2-dimensional fluid-attenuated inversion recovery images (10,000 ms, 140 ms, and 2200 ms for repetition time, echo time, and inversion time, respectively; matrix: 512 × 512; field of view: 240 × 240 mm^2) were collected and used for determination of white matter hyperintensity volume.

LA Volume and Number Analysis

The volume of LA was calculated using a semiautomated segmentation technique previously described[5] (Jim, Xinapse Systems, Leicester, UK). One experienced neuroradiologist (L.S.) performed the analysis by considering as LA hyperintense white matter regions on fluid-attenuated inversion recovery images not related to small or lacunar infarcts (patients with large-vessel infarcts were already excluded as stated in the exclusion criteria). LA was classified for each hemisphere (left or right) according to the vascular territories (anterior cerebral artery, middle cerebral artery, and posterior cerebral artery) and according to the involvement of the periventricular white matter or deep white matter. The volume was quantified in cubic centimeters. The software automatically calculated the volume after the identification of the areas of LA.

Statistical Analysis

The normality of each continuous variable group was tested using the Kolmogorov-Smirnov *Z* test. Continuous data were described as the mean value ± standard deviation, whereas non-Gaussian with median and percentiles. Pearson rho correlation analysis was performed to evaluate the association between the LA volume of the different territories and the different monochromatic energy levels (66, 70, 77, 86, 100, 140, 160, and 180 keV, and further with 100 and 140 kV) according to the type of plaque (fatty, mixed, or calcified). A *P* value <.05 was regarded to indicate statistically significant association. All *P* values were calculated using a 2-tailed significance level. Statistical analysis was performed with SPSS Statistics 18.0 (SPSS Inc, Chicago, IL). Graphics were plotted with MedCalc 15.0 software (MedCalc, Mariakerke, Belgium).

Results

General Results

No patients were excluded from the analysis because of suboptimal quality, and the demographic characteristics of the patients are given in Table 1. In Tables 2 and 3, the summary of LA distribution and HU attenuation according to the types of plaque is given.

Correlation Analysis

In Table 4, the results of correlation analysis are given. The presence of an inverse statistically significant correlation between the HU carotid artery plaque attenuation and the volume of the LA is clear. Because of the presence of calcified plaques, we calculated a second model by including only the fatty and mixed plaques, and the data are summarized in Table 5. In this case, we found that the association was observed while using keV levels from 66 to 86, and 100 kV.

Discussion

The ability to perform dual-energy scanning at CT is being developed by most CT scanner manufacturers because it provides the ability to differentiate between different materials. In the last years, several papers showed the potentiality of dual-energy analysis of the body tissues,[3,4] demonstrating that each tissue can have a specific signature owing to the intrinsic characteristics of the Compton

Table 1. *Demographic characteristics of the patients*

Age (y)	69 ± 19
Gender (male)	68% (34)
Previous TIA*	58% (29)
Previous CAD	42% (21)
Hypertension	56% (23)
Diabetes	18% (9)
Dyslipidemia	40% (20)

Abbreviations: CAD, coronary artery disease; TIA, transient ischemic attack.

*Stroke was an exclusion criterion.

Table 2. *Normality test and brain volume* and lesion distribution*

	Mean	95% CI	SD	Median	95% CI	2.5-97.5 P	Normal distr.
ACA lesions	4,118	3.276-4.959	42,828	3	2.000-4.000	.000-15.950	<.0001
ACA volume	372.118	291.248-452.988	411.7226	232	147.257-337.369	.000-1,408.600	<.0001
MCA lesions	8,225	6.823-9.628	71,406	5.5	5.000-8.000	.000-29.750	<.0001
MCA volume	1,143.422	887.591-1,399.252	1,302.476	543.5	453.000-872.984	.000-4,528.100	<.0001
PCA lesions	2,255	1.681-2.829	29,237	2	1.000-2.000	.000-7.000	<.0001
PCA volume	269.353	193.465-345.241	386.3597	122.5	41.626-213.374	.000-1,440.050	<.0001
Hemisphere lesions	14.598	12.447-16.750	10.9538	14	10.626-15.374	.000-42.850	.0001
Hemisphere Volume	1,784.892	1,445.590-2124.195	1,727.4456	1,340	865.076-1,776.828	.000-6,450.850	<.0001
PVWMH	1,278.902	993.736-1,564.068	1,451.8292	706	531.760-1,290.866	.000-5,461.750	<.0001
DWMH	505.99	418.861-593.119	443.5898	375	277.380-518.598	.000-1,475.000	.0051

Abbreviations: ACA, anterior cerebral artery; CI, confidence interval; DWMH, deep white matter hyperintensity; MCA, middle cerebral artery; PCA, posterior cerebral artery; PVWMH, periventricular white matter hyperintensity; SD, standard deviation.
*Expressed in cubic centimeters.

Table 3. *Normality test and plaque attenuation according to the energy level*

	Mean	95% CI	SD	Median	95% CI	2.5-97.5 P	Normal distr.
keV 66	372.999	263.811-482.187	564.2078	86	71.000-100.038	21.000-1854.000	<.0001
keV 70	346.821	245.784-447.858	522.0898	81	69.000-94.019	26.000-1720.000	<.0001
keV 77	312.03	221.996-402.065	465.2366	76	62.981-84.019	32.000-1535.000	<.0001
keV 86	277.852	198.323-357.381	410.9503	71	68.847-74.000	27.000-1364.000	<.0001
keV 100	243.93	174.917-312.942	356.6106	66	55.000-74.000	25.000-1190.000	<.0001
keV 140	201.9	145.872-257.928	289.5117	55	50.000-63.000	20.000-970.000	<.0001
keV 160	192.659	139.450-245.869	274.9495	54	50.000-60.000	17.125-924.000	<.0001
keV 180	186.391	135.006-237.777	265.5259	52	49.000-59.000	15.125-894.000	<.0001
kV 100	368.971	260.648-477.295	559.7403	85	70.000-98.019	23.000-1857.000	<.0001
kV 140	246.524	173.620-319.429	373.0271	67	57.000-75.846	21.000-1245.000	<.0001

Abbreviations: CI, confidence interval; SD, standard deviation.

and photoelectric effect.[2] Moreover, a second consequence owing to the introduction of DECT scanner was that it is possible to measure the attenuation value of a tissue by considering different keV levels[16,17] and by obtaining attenuation information that minimizes or maximizes (according to the used keV) the Compton and photoelectric effect. The extent of attenuation of an incident X-ray is determined by its energy and the properties of the intervening matter: its atomic composition (Z), density, and thicknesses. In particular, attenuation is strongly related to the Z-value, and it is typically higher for lower energy than for higher energy photons, where attenuation is related to the electron density. Therefore, a material will show different attenuation when imaged with multiple energy spectra. Algorithms that quantify radiation owing to the materials and in turn make up an image are called base material decomposition.

This approach allows testing the potential association of different HU values according to the keV used, and the purpose was to assess if there is a correlation between the carotid CT plaque attenuation values measured by DECT scanner and brain LA. The rationale of this study relies on the fact that the etiopathogenesis of LA is not completely understood,[7,11,12,18] and even if most authors suggest that LA is due to small-vessel pathology, other evidence seems to support the hypothesis that large-vessel pathology, namely carotid artery, is related to the development and severity of LA.

DECT allows a new type of carotid artery plaque imaging assessment, and the threshold analysis of attenuation,[5] due to the different keV values, could better characterize and confirm the association between some subtypes of atherosclerotic plaques and LA. In the design of this study, we searched for patients who underwent both DECT of carotid arteries and brain MR, with a time difference between these 2 procedures <3 months.

The assessment of the distribution of LA volume (Table 2) shows that most of the lesions and the volume involve the MCA territories for both right and left sides, and that the biggest amount of LA volume is localized in the periventricular white matter. By assessing the HU values according to the energy level, Table 3 shows that there is

Table 4. *Pearson rho correlation analysis (*P *value)*

		keV_66	keV_70	keV_77	keV_86	keV_100	keV_140	keV_160	keV_180	kV_100	kV140
ACA volume	rho	−0.346	−0.346	−0.347	−0.346	−0.345	−0.344	−0.343	−0.342	−0.343	−0.334
	P value	.0004	.0004	.0004	.0004	.0004	.0004	.0004	.0004	.0004	.0007
ACA lesions	rho	−0.309	−0.309	−0.31	−0.309	−0.308	−0.308	−0.307	−0.305	−0.307	−0.299
	P value	.0016	.0016	.0015	.0016	.0016	.0017	.0017	.0018	.0017	.0025
MCA volume	rho	−0.351	−0.35	−0.351	−0.349	−0.347	−0.344	−0.342	−0.341	−0.349	−0.337
	P value	.0003	.0003	.0003	.0003	.0004	.0004	.0004	.0005	.0003	.0006
MCA lesions	rho	−0.335	−0.334	−0.334	−0.333	−0.33	−0.326	−0.324	−0.323	−0.332	−0.32
	P value	.0006	.0006	.0006	.0006	.0007	.0008	.0009	.0009	.0006	.0012
PCA volume	rho	−0.26	−0.26	−0.261	−0.261	−0.261	−0.262	−0.262	−0.261	−0.258	−0.253
	P value	.0084	.0084	.008	.0081	.008	.0077	.0079	.0081	.0088	.0111
PCA lesions	rho	−0.151	−0.152	−0.155	−0.159	−0.162	−0.167	−0.168	−0.168	−0.151	−0.156
	P value	.1289	.126	.119	.111	.104	.0937	.0922	.0907	.1288	.12
Hemisphere volume	rho	−0.405	−0.405	−0.405	−0.404	−0.402	−0.4	−0.398	−0.397	−0.403	−0.392
	P value	<.0001	<.0001	<.0001	<.0001	<.0001	<.0001	<.0001	<.0001	<.0001	.0001
Hemisphere lesions	rho	−0.38	−0.379	−0.381	−0.38	−0.379	−0.377	−0.376	−0.375	−0.377	−0.369
	P value	.0001	.0001	.0001	.0001	.0001	.0001	.0001	.0001	.0001	.0002
Hemisphere PVWHM	rho	−0.37	−0.369	−0.37	−0.369	−0.368	−0.366	−0.365	−0.364	−0.367	−0.358
	P value	.0001	.0001	.0001	.0001	.0001	.0002	.0002	.0002	.0001	.0003
Hemisphere DWHM	rho	−0.367	−0.367	−0.367	−0.365	−0.363	−0.359	−0.357	−0.355	−0.365	−0.352
	P value	.0001	.0001	.0001	.0002	.0002	.0002	.0002	.0002	.0002	.0003

Abbreviations: ACA, anterior cerebral artery; MCA, middle cerebral artery; PCA, posterior cerebral artery.
P values <.05 are statistically significant.

Table 5. *Pearson Rho correlation analysis (*P *value) (excluding calcified plaques)*

		keV_66	keV_70	keV_77	keV_86	keV_100	keV_140	keV_160	keV_180	kV_100	kV_140
ACA volume	rho	−0.133	−0.131	−0.124	−0.097	−0.055	−0.012	−0.005	0.002	−0.128	−0.065
	P value	.2683	.2766	.304	.4188	.6463	.9207	.9697	.9885	.2868	.5895
ACA lesions	rho	−0.04	−0.035	−0.023	−0.007	0.015	0.025	0.027	0.03	−0.037	0.001
	P value	.7408	.773	.8486	.9516	.9029	.8347	.8252	.8064	.7612	.9909
MCA volume	rho	−0.245	−0.261	−0.277	−0.252	−0.197	−0.114	−0.101	−0.096	−0.241	−0.212
	P value	.0398	.0281	.0196	.0341	.0998	.3433	.4018	.4269	.0433	.0763
MCA lesions	rho	−0.271	−0.282	−0.283	−0.242	−0.168	−0.076	−0.063	−0.056	−0.266	−0.188
	P value	.022	.0173	.0169	.042	.1622	.528	.6001	.6449	.0248	.1171
PCA volume	rho	−0.078	−0.086	−0.094	−0.085	−0.071	−0.051	−0.043	−0.037	−0.079	−0.076
	P value	.5188	.4743	.4342	.4819	.5551	.6749	.7243	.7575	.5112	.5292
PCA lesions	rho	−0.07	−0.102	−0.153	−0.192	−0.207	−0.193	−0.186	−0.183	−0.081	−0.194
	P value	.5646	.3995	.202	.1084	.0832	.1071	.1207	.1261	.5037	.1043
Hemisphere volume	rho	−0.242	−0.256	−0.269	−0.241	−0.184	−0.104	−0.09	−0.083	−0.238	−0.199
	P value	.0418	.031	.0234	.0431	.1241	.3878	.455	.4906	.0455	.0956
Hemisphere lesions	rho	−0.217	−0.231	−0.241	−0.219	−0.165	−0.096	−0.084	−0.077	−0.215	−0.18
	P value	.0694	.053	.0427	.0665	.1698	.4282	.4843	.5216	.0715	.1334
Hemisphere PVWHM	rho	−0.181	−0.192	−0.206	−0.186	−0.147	−0.089	−0.078	−0.072	−0.175	−0.155
	P value	.1314	.1083	.0855	.1203	.2204	.4626	.5195	.549	.1455	.1959
Hemisphere DWHM	rho	−0.339	−0.355	−0.359	−0.316	−0.225	−0.109	−0.091	−0.082	−0.344	−0.257
	P value	.0038	.0024	.0021	.0074	.0592	.3661	.4518	.4977	.0033	.0306

Abbreviations: ACA, anterior cerebral artery; MCA, middle cerebral artery; PCA, posterior cerebral artery.
P values <.05 are statistically significant.

an inverse correlation between the HU values and the keV values (by considering these between 66 keV and 180 keV).

Table 4 shows the results of correlation analysis. It is clear that there is a presence of an inverse statistically significant correlation between the HU carotid artery plaque attenuation and the volume of the LA. Because of the presence of calcified plaques, we calculated a second model by including only the fatty and mixed plaques, and the data are summarized in Table 5. In this case, we found that the association was observed using only low keV

levels from 66 to 86, and 100 kV. This is an interesting finding because this suggests that some features that are more visible with low energy levels are more frequently associated with the presence of LA.

A recently published systematic review and meta-analysis suggested that LA has a tendency of association with carotid plaques, but no association with simple carotid stenosis was found.[19] The plaque composition and structure could be a marker for the presence and severity of LA. In the physics of DECT, it was demonstrated that the iodine (contrast medium) attenuation is highly dependent on the keV values (with an inverse correlation function),[20,21] and therefore our results could be explained by the fact that the patients with an increased volume of LA have in their plaques an increased amount of contrast material molecules. This observation could support the hypothesis that the etiology of LA could be due to an atherosclerotic process[22] that involves not only the small vessels but also the large vessels. In particular, the presence of iodine in the plaque is mainly due to neovascularization,[23,24] and it could be associated with an increased, systemic atherosclerotic activity as demonstrated in a recent published study that demonstrated the association between carotid plaque features and increased risk of myocardial infarction.[25] Following this hypothesis, the presence of atherosclerotic disease, with plaques that show contrast (detected with the keV variation), could be considered as a surrogate marker of LA.

It is important to underline that differences in HU measurements of carotid plaque reflect pathological differences that could lead to an increased risk of stroke,[26] by suggesting a common pathway between risk of stroke and LA. This hypothesis is concordant with previous observation that found that subjects with LA have an increased risk of stroke.[27,28]

However, the main target of this study was to identify the possible link between plaque electronic density (as reflected by CT attenuation) and white matter pathology. In the past years, although carotid atherosclerosis has been demonstrated to have a strong relationship with stroke and small-vessel disease, its association with LA was controversial,[29,30] but some years later, there was a shift in the point of view because other studies, mainly performed with MRI technique, found an association between the presence of the atherosclerotic load in the carotid artery plaque and the presence and severity of white matter changes.[31,32] However, the association between atherosclerosis and white matter pathology was not clear because it is well known that there are several types of atherosclerosis,[33] and some authors found an association between the presence of calcium components and LA,[34] whereas others found an association between lipid components and LA,[13] which are 2 completely different types of plaque. Regarding this point, it would be important to remember that the pathogenesis of atherosclerosis and cerebral small-vessel disease is associated with inflammatory process,[35,36] and also plays a role in the response to ischemic events that result from atherosclerosis.[36]

We think that the explanation of our results could be possible by considering this hypothesis: that LA and atherosclerosis share a common pathway: the inflammation, and that the inflammatory presence (and severity) in the carotid artery plaques (usually associated with the fatty subtype) could be well detected by applying the multi-energy CT approach because of the excellent attenuation of the iodium (the main component of the iodinated contrast material) with the variation of the keV.[37]

This hypothesis is strengthened by the fact that some studies have found a direct relationship between the amount of the contrast that enters into a carotid artery plaque (the carotid plaque enhancement) and the micro-vessel density and degree of inflammation.[23,24,38]

We are aware that this study has some limitations. The first one is its retrospective design. A prospective analysis could offer more reliable results; however, we think that this could be considered a minor limitation because of the type of investigation of the study. The second limitation is the relatively small number of analyzed patients. The third one is that it lacks histopathological confirmation that would represent the reference standard for the plaque composition.

Conclusion

In conclusion, the results of our study suggest that the associations between HU attenuation of the carotid artery plaques (with the exclusion of calcified plaques) and the volume of LA are emphasized at low keV energy levels. The diagnostic implication of these results is that the DECT of the carotid artery plaque could be useful not only to identify the plaque composition but also to characterize some features that are associated with the vascular degeneration of the brain such as the LA.

References

1. Haghighi RR, Chatterjee S, Vyas A, et al. X-ray attenuation coefficient of mixtures: inputs for dual-energy CT. Med Phys 2011;38:5270-5279. doi:10.1118/1.3626572. PMID 21992344.
2. Gabbai M, Leichter I, Mahgerefteh S, et al. Spectral material characterization with dual-energy CT: comparison of commercial and investigative technologies in phantoms. Acta Radiol 2015;56:960-969. doi:10.1177/0284185114545150. [2014 Sep 2]; PMID 25182803. Epub.
3. Coursey CA, Nelson RC, Boll DT, et al. Dual-energy multidetector CT: how does it work, what can it tell us, and when can we use it in abdominopelvic imaging? Radiographics 2010;30:1037-1055. doi:10.1148/rg.304095175. PMID 20631367.
4. Ameli-Renani S, Rahman F, Nair A, et al. Dual-energy CT for imaging of pulmonary hypertension: challenges and opportunities. Radiographics 2014;34:1769-1790. doi:10.1148/rg.347130085. PMID 25384277.
5. Saba L, Argiolas GM, Siotto P, et al. Carotid artery plaque characterization using CT multienergy imaging. AJNR

Am J Neuroradiol 2013;34:855-859. doi:10.3174/ajnr.A3285. [2012 Oct 4]; PMID 23042919. Epub.
6. Pantoni L. Leukoaraiosis: from an ancient term to an actual marker of poor prognosis. Stroke 2008;39:1401-1403. doi:10.1161/STROKEAHA.107.505602. [2008 Mar 13]; PMID 18340098. Epub.
7. Pantoni L, Inzitari D. New clinical relevance of leukoaraiosis. European Task Force on Age-Related White Matter-Changes. Stroke 1998;29:543. PMID 9472903.
8. Pantoni L, Garcia JH. Pathogenesis of leukoaraiosis: a review. Stroke 1997;28:652-659. PMID 9056627. Review.
9. Jokinen H, Gonçalves N, Vigário R, et al. Early-stage white matter lesions detected by multispectral MRI segmentation predict progressive cognitive decline. Front Neurosci 2015;9:455. doi:10.3389/fnins.2015.00455. eCollection 2015, PMID 26696814. PubMed Central PMCID: PMC4667087.
10. Jokinen H, Schmidt R, Ropele S, et al. Diffusion changes predict cognitive and functional outcome: the LADIS study. Ann Neurol 2013;73:576-583. doi:10.1002/ana.23802. [2013 Feb 19]; PMID 23423951. Epub.
11. Lambert C, Benjamin P, Zeestraten E, et al. Longitudinal patterns of leukoaraiosis and brain atrophy in symptomatic small vessel disease. Brain 2016; 139(Pt 4):1136-1151. doi:10.1093/brain/aww009. [2016 Mar 1];PMID 26936939. Epub, PubMed Central PMCID: PMC4806220.
12. Lucatelli P, Raz E, Saba L, et al. Relationship between leukoaraiosis, carotid intima-media thickness and intima-media thickness variability: preliminary results. Eur Radiol 2016;[2016 Mar 30]; PMID 27027314. Epub ahead of print.
13. Saba L, Raz E, Grassi R, et al. Association between the volume of carotid artery plaque and its subcomponents and the volume of white matter lesions in patients selected for endarterectomy. AJR Am J Roentgenol 2013;201:W747-W752. doi:10.2214/AJR.12.10217. PMID 24147504.
14. Saba L, Sanfilippo R, Pascalis L, et al. Carotid artery abnormalities and leukoaraiosis in elderly patients: evaluation with MDCT. AJR Am J Roentgenol 2009;192: W63-W70. doi:10.2214/AJR.07.3566. PMID 19155382.
15. de Weert TT, Ouhlous M, Zondervan PE, et al. In vitro characterization of atherosclerotic carotid plaque with multidetector computed tomography and histopathological correlation. Eur Radiol 2005;15:1906-1914.
16. Faby S, Kuchenbecker S, Sawall S, et al. Performance of today's dual energy CT and future multi energy CT in virtual non-contrast imaging and in iodine quantification: a simulation study. Med Phys 2015;42:4349-4366. doi:10 .1118/1.4922654. PMID 26133632.
17. Maass C, Baer M, Kachelriess M. Image-based dual energy CT using optimized precorrection functions: a practical new approach of material decomposition in image domain. Med Phys 2009;36:3818-3829. PMID 19746815.
18. Opherk C, Gonik M, Duering M, et al. Genome-wide genotyping demonstrates a polygenic risk score associated with white matter hyperintensity volume in CADASIL. Stroke 2014;45:968-972. doi:10.1161/STROKEAHA.113 .004461. [2014 Feb 27]; PMID 24578207. Epub.
19. Liao SQ, Li JC, Zhang M, et al. The association between leukoaraiosis and carotid atherosclerosis: a systematic review and meta-analysis. Int J Neurosci 2015;125:493-500.
20. Tran DN, Straka M, Roos JE, et al. Dual-energy CT discrimination of iodine and calcium: experimental results and implications for lower extremity CT angiography. Acad Radiol 2009;16:160-171. doi:10.1016/j.acra.2008.09.004. PMID 19124101.
21. Shikhaliev PM. Energy-resolved computed tomography: first experimental results. Phys Med Biol 2008;53:5595-5613. doi:10.1088/0031-9155/53/20/002. [2008 Sep 17]; PMID 18799830. Epub.
22. Li H, Xu G, Xiong Y, et al. Relationship between cerebral atherosclerosis and leukoaraiosis in aged patients: results from DSA. J Neuroimaging 2014;24:338-342. doi:10.1111/ jon.12047. [2013 Sep 3]; PMID 24033698. Epub.
23. Saba L, Lai ML, Montisci R, et al. Association between carotid plaque enhancement shown by multidetector CT angiography and histologically validated microvessel density. Eur Radiol 2012;22:2237-2245.
24. Saba L, Piga M, Raz E, et al. Carotid artery plaque classification: does contrast enhancement play a significant role? AJNR Am J Neuroradiol 2012;33:1814-1817.
25. Mosleh W, Adib K, Natdanai P, et al. High-risk carotid plaques identified by CT-angiogram can predict acute myocardial infarction. Int J Cardiovasc Imaging 2016;[2016 Nov 19]; PMID 27866279. Epub ahead of print.
26. Gupta A, Baradaran H, Mtui EE, et al. Detection of symptomatic carotid plaque using source data from MR and CT angiography: a correlative study. Cerebrovasc Dis 2015;39:151-161.
27. Smith EE. Leukoaraiosis and stroke. Stroke 2010;41(10 Suppl):S139-S143.
28. Kim GM, Park KY, Avery R, et al. Extensive leukoaraiosis is associated with high early risk of recurrence after ischemic stroke. Stroke 2014;45:479-485.
29. Manolio TA, Burke GL, O'Leary DH, et al. Relationships of cerebral MRI findings to ultrasonographic carotid atherosclerosis in older adults: the Cardiovascular Health Study. CHS Collaborative Research Group. Arterioscler Thromb Vasc Biol 1999;19:356-365.
30. de Leeuw FE, de Groot JC, Bots ML, et al. Carotid atherosclerosis and cerebral white matter lesions in a population based magnetic resonance imaging study. J Neurol 2000;247:291-296.
31. Pico F, Dufouil C, Lévy C, et al. Longitudinal study of carotid atherosclerosis and white matter hyperintensities: the EVA-MRI cohort. Cerebrovasc Dis 2002;14:109-115.
32. Shrestha I, Takahashi T, Nomura E, et al. Association between central systolic blood pressure, white matter lesions in cerebral MRI and carotid atherosclerosis. Hypertens Res 2009;32:869-874.
33. Holmstedt CA, Turan TN, Chimowitz MI. Atherosclerotic intracranial arterial stenosis: risk factors, diagnosis, and treatment. Lancet Neurol 2013;12:1106-1114. doi:10.1016/ S1474-4422(13)70195-9.
34. Chung PW, Park KY, Moon HS, et al. Intracranial internal carotid artery calcification: a representative for cerebral artery calcification and association with white matter hyperintensities. Cerebrovasc Dis 2010;30:65-71.
35. Ross R. Atherosclerosis—an inflammatory disease. N Engl J Med 1999;340:115-126.
36. van Dijk EJ, Prins ND, Vermeer SE, et al. C-reactive protein and cerebral small-vessel disease: the Rotterdam Scan Study. Circulation 2005;112:900-905.
37. Primak AN, Ramirez Giraldo JC, Liu X, et al. Improved dual-energy material discrimination for dual-source CT by means of additional spectral filtration. Med Phys 2009;36:1359-1369.
38. Gaemperli O, Shalhoub J, Owen DR, et al. Imaging intraplaque inflammation in carotid atherosclerosis with 11C-PK11195 positron emission tomography/computed tomography. Eur Heart J 2012;33:1902-1910.